Atmos. Chem. Phys. Discuss., doi:10.5194/acp-2016-582, 2016
Manuscript under review for journal Atmos. Chem. Phys.
Published: 20 July 2016

Atmospheric Chemistry and Physics Discussions

Influence of enhanced Asian NO_x emissions on ozone in the Upper Troposphere and Lower Stratosphere (UTLS) in chemistry climate model simulations

Chaitri Roy[1], Suvarna Fadnavis[1], Rolf Müller[2,] Ayantika Dey Chaudhary[1] and Felix Ploeger[2]

[1]Indian Institute of Tropical Meteorology, Pune, India

[2]Forschungszentrum Jülich GmbH, IEK7, Jülich, Germany

Email of corresponding author: suvarna@tropmet.res.in

Abstract:

Asian summer monsoon convection plays an important role in efficient vertical transport from the surface to the anticyclone. In this paper we investigate the potential impact of convectively transported anthropogenic nitrogen oxides (NO_x) on the distribution of ozone in the Upper Troposphere and Lower Stratosphere (UTLS) from simulations with the fully-coupled aerosol chemistry climate model, ECHAM5-HAMMOZ. We performed anthropogenic NO_x emission sensitivity experiments over India and China. In these simulations, anthropogenic NO_x emissions for the period 2000-2010 have been increased by 38% over India and by 73% over China in accordance with satellite observed trends over India of 3.8 % per year and China of 7.3% per year. These NO_x emission sensitivity simulations show that strong convection over the Bay of Bengal and the Southern slopes of the Himalayas transports Indian emissions into the UTLS. Convective transport from the South China Sea injects Chinese emissions into the lower stratosphere. Indian and Chinese emissions are partially transported over the Arabian Sea and west Asia by the tropical easterly jet. Enhanced NO_x emissions over India and China increase the ozone radiative forcing over India by 0.112 W/m^2 and 0.121 W/m^2 respectively. These elevated emissions produces significant warming over the Tibetan Plateau and increase precipitation over India due to a strengthening of the monsoon Hadley circulation.

However doubling of NO_x emissions over India (73%); equal to China, produced high ozone in the

Atmos. Chem. Phys. Discuss., doi:10.5194/acp-2016-582, 2016
Manuscript under review for journal Atmos. Chem. Phys.
Published: 20 July 2016

Atmospheric Chemistry and Physics Discussions

lower troposphere. It induced a reverse monsoon Hadley circulation and negative precipitation anomalies over India. The associated subsidence suppressed vertical transport of NO_x and ozone into the anticyclone.

Key words: Asian summer monsoon, Ozone, increase in tropospheric NO_x, NO_x transport, Upper troposphere and lower stratosphere.

1. Introduction

Rapid economic development and urbanization in Asia has resulted in an unprecedented growth in anthropogenic emissions like nitrogen oxides (NO_x), carbon monoxide (CO), carbon dioxide (CO_2), methane (CH_4,), etc. Many of these species have implications on tropospheric ozone (Wild and Akimoto, 2001; IPCC, 2001). Ground based and satellite observations show a high amount of these ozone precursors concentrated over the India and China (Sinha et al., 2014; Richter et al., 2005; Jacob et al., 1999; Zhao et al., 2013; Gu et al., 2014). Recent studies show that tropospheric ozone production over Asia is controlled by the abundance of NO_x and VOCs and the ratios of these species (Sillman, 1995, Lei et al., 2004, Zhang et al., 2004 and Tie et al., 2007). These studies reveal that in Asia, particularly India and China are NO_x limited regions, i.e., controlling NOx in these regions would reduce ozone concentrations (Yamaji et al., 2006; Sinha et al., 2014; Fadnavis et al., 2014). Thus levels of tropospheric ozone, a key polluting agent and greenhouse gas, are controlled by NO_x concentration over these regions. Recently, a positive trend of 3.8 % yr^{-1} (for the period 2003-2011) in tropospheric column NO_2 over India has been reported using SCanning Imaging Absorption SpectroMeter for AtmosphericCHartographY (SCIAMACHY) observations (Ghude et al., 2013) and of 7.3% yr^{-1} (for the period 2002-2011) over China from Ozone Monitoring Instrument (OMI) observations (Schneider and van der A, 2012). Apart from anthropogenic sources, lightning also contributes to the production of NOx. Over the Asian region, in the middle and upper troposphere, lightning contributes ~40% to NO_x

Atmos. Chem. Phys. Discuss., doi:10.5194/acp-2016-582, 2016
Manuscript under review for journal Atmos. Chem. Phys.
Published: 20 July 2016

Atmospheric Chemistry and Physics Discussions

and 20% to ozone production during monsoon season (Tie et al 2001; Fadnavis et al 2015). The upper tropospheric ozone concentration is determined both by in-situ production as well as from convective transport from the boundary layer (Søvde et al., 2011).

Ozone in the troposphere absorbs relatively little UV radiation but it has a huge climatic impact (Lacis et al., 1990). The estimated global average radiative forcing increasing tropospheric ozone since pre-industrial times is estimated to be $+0.35 \pm 0.15$ Wm^{-2} (IPCC, Ramaswamy et al., 2001). Previous studies revealed that ozone perturbations exert a large influence on temperature near the surface and tropopause (e.g., Thuburn and Craig, 2002; Foster and Shine 1997). Thus the tropospheric ozone distribution and its variability at different altitudes influence the thermal structure of the atmosphere. Climate change due to ozone variations is highest near the tropopause because the greenhouse efficiency per molecule is highest there (Lacis et al, 1990; Forster and Shine, 1997; Riese et al., 2012). A study based on ACCMIP models reports that NO_X and CH_4 are the greatest contributors in determining ozone radiative forcing (Stevenson et al., 2013).

Asian Summer Monsoon (ASM) convection efficiently transports Asian pollutants from the boundary layer into the Upper Troposphere and Lower Stratosphere (UTLS) (Randel and Park, 2006; Randel et al. 2010; Fadnavis et al., 2013, 2015). Studies pertaining to modeling and trajectory analysis confirm this finding (Li et al., 2005; Park et al., 2007; Randel et al., 2010; Chen et al., 2012; Vogel et al., 2015). Satellite observations show the confinement of a number of chemical constituents like water vapor (H_2O), CO, ethane (C_2H_6), CH_4, nitrous oxide (N_2O), hydrogen cyanide (HCN), and aerosols, within the ASM anticyclone (Randel et al. 2010; Li et al., 2005; Randel and Park, 2006; Lawrence et al., 2011) which has potential implication on stratospheric chemistry and dynamics. These studies indicate that the rise in anthropogenic emissions over the ASM region alters the chemical composition of the UTLS (Lawrence et al., 2011; Fadnavis et al, 2014, 2015) during the monsoon season. Another prominent feature of the satellite observations is an ozone minimum in the ASM anticyclone (near 100

Atmos. Chem. Phys. Discuss., doi:10.5194/acp-2016-582, 2016
Manuscript under review for journal Atmos. Chem. Phys.
Published: 20 July 2016

Atmospheric Chemistry and Physics Discussions

hPa) (Gettelman et al., 2004; Konopka et al., 2010; Braesicke et al., 2011). This ozone minimum is linked to ozone poor air masses arriving from the Bay of Bengal and Arabian Sea. Balloonsonde observations show that ozone variations near the anticyclone are strongly correlated with temperature near the tropopause (Tobo et al., 2008). Thus observations show that convectively lifted air masses arriving in the anticyclone are ozone poor but rich in ozone precursors. Thus the linkage of low ozone and high ozone precursors with temperature variation in the anticyclone is an open question. In this study we ask the question 'how do rising Asian NO_X (an important ozone precursor) emissions and associated ozone production affect the ozone radiative forcing and monsoon circulation?' For this we perform anthropogenic NO_x emission sensitivity experiments using the state-of-the-art ECHAM5-HAMMOZ (European Centre General Circulation Model version5) chemistry climate model (Roeckner et al., 2003; Horowitz et al., 2003; Stier et al., 2005). From these simulations ozone radiative forcing for different anthropogenic NO_x emission scenarios is estimated. Associated temperature and monsoon circulation changes are also reported. The paper is organized as follows: data description and model setup are discussed in section 2; results are discussed in section 3. Section 4 comprises of discussion followed by conclusion in section 5.

2. Data description and Model setup

2.1 Satellite measurement

Earth Observing System (EOS) microwave limb sounder (MLS) is a NASA Aura satellite which flies in the polar sun-synchronous orbit. It measures the thermal emissions at millimeter and sub-millimeter wavelengths (Waters et al., 2006). It performs 240 limb scans per orbit with a footprint of ~6 km across-track and ~200 km along-track, providing ~3500 profiles per day. MLS also measures the vertical profiles of temperature, ozone, CO, H_2O, and many other constituents in the mesosphere, stratosphere and upper troposphere (Waters et al., 2006). In the UTLS, MLS has a vertical resolution of

Atmos. Chem. Phys. Discuss., doi:10.5194/acp-2016-582, 2016
Manuscript under review for journal Atmos. Chem. Phys.
Published: 20 July 2016

Atmospheric Chemistry and Physics Discussions

3 km. MLS vertical profiles of ozone show good agreement with the Stratospheric Aerosol and Gas Experiment II (SAGE-II), Halogen Occultation Experiment (HALOE), Atmospheric Chemistry Experiment (ACE) and ozonesonde measurements (Froidevaux et al.,2006). The MLS ozone profiles are considered to be useful in the range of 215 – 0.46 hPa (Livesey et al., 2005). In this study we analyze the MLS level 2 (version 4) ozone mixing ratios data for the period 2004 – 2013. The data has been gridded at 8.3ºx3º. This data can be accessed from http://mls.jpl.nasa.gov/. For comparison simulated ozone is convolved with the MLS averaging kernel. Details of MLS averaging kernels are documented by Livesey et al. (2011).

2.2 Model simulation and experimental setup

We employ the aerosol-chemistry-climate model ECHAM5-HAMMOZ which comprises the general circulation model ECHAM5 (Roeckner et al., 2003), the tropospheric chemistry module, MOZ (Horowitz et al 2003) and the aerosol module, Hamburg aerosol model (HAM) (Stier et al., 2005). It includes NO_x, VOC and aerosol chemistry. The gas phase chemistry is based on the chemical scheme provided by the MOZART-2 model (Horowitz et al., 2003) which includes detailed chemistry of the O_X-NO_X hydrocarbon system with 63 tracers and 168 reactions. The $O(^1D)$ quenching reaction rates were updated according to Sander et al., (2003) and isoprene nitrates chemistry according to Fiore et al., (2005). The dry deposition in ECHAM5-HAMMOZ follows the scheme given by Ganzeveld and Lelieveld (1995). Soluble trace gases like HNO_3 and SO_2 are also subject to wet deposition. In-cloud and below-cloud scavenging follows the scheme given by Stier et al. (2005).

The model is run at a T42 spectral resolution corresponding to about 2.8°×2.8° in the horizontal dimension and 31 vertical hybrid σ – p levels from the surface to 10 hPa. The details of model parameterizations, emissions and validation are described by Fadnavis et al. (2013; 2014; 2015) and Pozzoli et al. (2008a, b; 2011). The base year for trace gas emissions is taken as 2000. Each member of

Atmos. Chem. Phys. Discuss., doi:10.5194/acp-2016-582, 2016
Manuscript under review for journal Atmos. Chem. Phys.
Published: 20 July 2016

Atmospheric Chemistry and Physics Discussions

121 our sensitivity study consists of continuous simulations for eleven years from 2000 to 2010. For each
122 simulation emissions were the same. Meteorology varied due to varying sea surface temperature (SST)
123 and sea ice (SIC). The AMIP2 SSTs and SIC representative of the period 2000 – 2010 were specified as
124 a lower boundary condition.

125 In order to understand the impact of increasing NO_x emissions on the distribution of ozone in
126 the UTLS, simulations were performed for the period 2000 – 2010. The experimental set up is the same
127 as described by Fadnavis et al., (2015). The four experiments analyzed in this study are (1) A reference
128 experiment (CTRL) and three sensitivity experiments (referred to as experiments 2 - 4), where the NO_X
129 emissions over India and China are scaled in accordance with the observed trends. In experiment (2),
130 NO_X emissions are increased over India by 38% (Ind38), in experiment (3) increases that over China
131 by 73% (Chin73) are prescribed. In order to analyze the effects of equal NO_x emissions over India and
132 China, NO_x emissions are increased over India by 73% over India (Ind73) in experiment (4). The
133 emission perturbations were obtained from observed NO_2 trends of 3.8% per year over India (Ghude et
134 al., 2013) and 7.3% per year over China (Schneider and van der A, 2012). Hiboll et al., (2013) also
135 reported similar increasing NO_x values over megacities in India and China.

136 To calculate the heating associated with ozone changes over India and China, we use the
137 radiative transfer model Santa Barbara DISORT Atmospheric Radiative Transfer (SBDART). This
138 model is designed and developed by the University of California, Santa Barbara (Ricchiazzi et al.,
139 1998) and is based on a collection of well-tested and reliable physical models. We used eight streams in
140 the radiative transfer calculation and computations were made for solar zenith angles at every 5°.

141

142 **3. Results**

143 **3.1 Comparison with AIRS satellite measurements in the UTLS**

144 Figure 1(a) shows the spatial distribution of MLS ozone mixing ratios at 100 hPa. The

Atmos. Chem. Phys. Discuss., doi:10.5194/acp-2016-582, 2016
Manuscript under review for journal Atmos. Chem. Phys.
Published: 20 July 2016

distribution of simulated ozone mixing ratios at the nearest model level, 90 hPa is plotted in figure 1(b). ECHAM5-HAMMOZ simulation is smoothed with averaging kernel of MLS. The winds plotted in figure 1(a) and 1 (b) show the extent of the monsoon anticyclone (20°E-120°E). Winds plotted in figure 1(b) depict the extent of the monsoon anticyclone (20°E-120°E). The spatial pattern of low ozone concentrations in the monsoon anticyclone is well simulated in the model. In the recent past, low ozone mixing ratios (~40-160 ppbv) in the monsoon anticyclone have been reported from MLS (90-140 ppbv), MIPAS (80-120 ppbv), SAGE II (<150ppbv) measurements (Kunze et al., 2010; Randel et al., 2001; Randel and Park 2006; Park et al., 2007). Vertical profiles of ozonesonde (averaged for the monsoon season during 2001-2009) at Indian stations, Delhi (28.61ºN, 77.23ºE), Pune (18.52ºN, 73.85ºE) and Thiruvananthapuram (8.48ºN, 76.95E) are compared with MLS measurements and ECHAM5-HAMMOZ simulated ozone mixing ratios in figures 1(c)-(e). These figures depict that vertical variation of simulated ozone show good agreement with ozonesonde and MLS observations. Fadnavis et al., (2015) compared the model simulation with aircraft observations over the various regions all over the globe during the monsoon season. This study reported a reasonable agreement for PAN, NOx, HNO_3 and ozone mixing ratio.

3.2 Transport of enhanced NO_x emissions into the UTLS

Recent satellite observations and model simulations established the impact of convective transport of boundary layer pollution into the ASM anticyclone during the Asian monsoon season (Gettelman et al., 2004; Randel et al., 2010; Fadnavis et al., 2013, 2014, 2015). These pollutants are further transported across the tropopause as evident in satellite observations of, e.g. water vapour (Bian, 2012), hydrogen cyanide (HCN) (Randel, 2010), CO (Schoeberl et al., 2006), Peroxyacetyl nitrate (PAN), aerosols (Vernier et al., 2015, Fadnavis et al 2013) etc. To understand the influence of monsoon convection on the vertical distribution of NO_x we show zonal and meridional cross sections over India

Atmos. Chem. Phys. Discuss., doi:10.5194/acp-2016-582, 2016
Manuscript under review for journal Atmos. Chem. Phys.
Published: 20 July 2016

and China. The vertical distribution of NO_x averaged for the monsoon season over the Indian latitudes (8°-35°N), and Chinese latitudes (20°-40°N) as obtained from CTRL simulations is shown in the supplementary figures S1(a) and S1(b) respectively. These figures show elevated levels of NO_x extending from the surface to the upper troposphere (UT) over India and China. The wind vectors along with the distribution of cloud droplet number concentration and ice crystal number concentration together, (Figure S2(a) and S2(b)) indicate strong convective transport from the Bay of Bengal (BOB), southern slopes of Himalayas, and south China Sea which might lift the boundary layer NO_x to the upper troposphere.

During the monsoon season, the NO_x distribution in the UTLS is influenced by lightning apart from transport from anthropogenic sources. In this season, lightning activity is highest in Asia (Ranalkar and Chaudhari, 2009; Penki and Kamra, 2013) compared to the other monsoon regions (North America, South America and Africa). However, in our simulations there is no contribution from lightning.

We show longitude-pressure (Figures 2(a)-(c)) and latitude-pressure sections (Figures 2(d)-(f)) of anomalies of anthropogenic NO_x obtained from Ind38, Ind73, Chin73 with respect to CTRL simulations. The black arrows indicate the anomalies of wind vectors. Ind38 and Chin73 simulations (Figures 2(a) and 2(d)) show that the convective winds at the southern flank of the Himalayas (80º-90°E) and over the Bay of Bengal lift up the enhanced NO_x emissions to the upper troposphere (UT). The majority of the outflow is into the UT and only part of it is transported into the lower stratosphere. Cross tropopause transport due to convection over South China Sea is evident in the Chin73 simulation (Figure 2(c) and 2(f)). Previous studies also indicate significant vertical transport due to strong monsoon convection from the southern slopes of Himalayas (Fu et al., 2006, Fadnavis et al., 2013; 2014) and the South China sea (Park et al 2009; Chen et al., 2012), which is in agreement with our results. In the upper troposphere, NO_x is transported over Iran and Saudi Arabia along the descending

Atmos. Chem. Phys. Discuss., doi:10.5194/acp-2016-582, 2016
Manuscript under review for journal Atmos. Chem. Phys.
Published: 20 July 2016

193 branch of circulation.

194 However the simulation with doubled NO_x emissions over India (Ind73) does not show cross
195 tropopause transport. The wind anomalies show a descending branch over central India (~20°N, 75°E)
196 (Figures 2(b) and 2(e)) which might have inhibited the cross-tropopause transport in the Ind73
197 simulation. The descending wind anomalies may be related to ozone radiative forcing and associated
198 temperature changes (discussed later in section 4).

199 Figures 2(d) and 2(f) also indicate transport of NO_x from India and China across the tropopause
200 and entrainment into the tropical pipe. Garny and Randel (2013) and Randel et al. (2010) also reported
201 that pollution transported by Asian monsoon convection enters the deep stratosphere via the tropical
202 pipe.

203

204 **3.3 Impact of enhanced anthropogenic NO_x on the tropospheric ozone distribution**

205 Tropospheric ozone is a radiatively active trace gas (Ramanathan et al., 1987) therefore it is
206 important to know the impact of enhanced NO_x emissions on tropospheric ozone production (Derwent,
207 1990). We estimate the change in ozone production due to enhanced NO_x emissions in the Ind38, Ind73
208 and Chin73 simulations with respect to CTRL. The longitude-pressure cross sections of changes in
209 amount of net ozone production (%) over India and China are shown in figures 3(a)-(c). It can be seen
210 that at the altitudes below 300 hPa there is ozone production and loss varying in between -60% to
211 +60%. In the upper troposphere (300-150hPa), the estimated amount of net ozone production in Ind38
212 and Ind73 simulation is ~5-10% and that from Chin73 simulation is ~10-30%. Comparison of figures 2
213 and 3 show that ozone production by NO_x photolysis occur in the regions where there is a transport of
214 NO_x. In Ind73 simulation there is no change in ozone production near the tropopause as the NO_x
215 emissions do not reach up to these altitudes (Figures 2(b) and 2(e)). In the Ind73 simulation there is
216 significant increase in net ozone production (~40-90% between 1000-500 hPa) over the Indo Gangetic

Atmos. Chem. Phys. Discuss., doi:10.5194/acp-2016-582, 2016
Manuscript under review for journal Atmos. Chem. Phys.
Published: 20 July 2016

Plain (figure not included).

Figures 4(a)-(c) show the longitude-pressure distribution of ozone mixing ratio anomalies obtained from Ind38 and Ind73 averaged over 8°-35°N, and Chin73 over 20°-45°N. Although the air mass in the monsoon anticyclone is poor in ozone (Figure 1(b)), the elevated ozone anomalies in response to increased NO_x emissions are seen in figure 4 (in the Ind38 and Chin73 simulations). This may be partially due to transported ozone via ASM convection and partially due to production of ozone (Figures 3 and 4); there is no contribution from lightning in our simulations. It can be seen from figures 4(a)-(c) that ozone levels are enhanced near 300-200 hPa over Arabia. This may be due to the ASM vertical convective transport and subsequent horizontal transport in the monsoon anticyclone (Randel et al., 2010, Garny and Randel, 2013; Vogel et al., 2015).

Latitude-pressure cross section of ozone anomalies plotted in figures 4(d) and 4(f) show that convection over the Bay of Bengal, southern slopes of the Himalayas and the South China Sea lifts ozone from India and China into the upper troposphere and it is then transported across the tropopause into the tropical pipe. Ozone and NO_x transported across the tropopause will enhance their amount in the surf mixing zone above the tropopause (Vogel et al., 2015). In the lower stratosphere there will be ozone production by photolysis from transported NO_x.

Doubling of NO_x emissions over India (Ind73) results in a descending branch of circulation over central India (Figures 4(b) and 4(e)). This subsidence suppressed the vertical transport of ozone across the tropopause. It is also evident in NO_x distribution (Figures 2(b) and 2(e)). As discussed earlier, this subsidence may be related to temperature changes due to ozone radiative forcing and heating rates as there is significant increase in ozone production over the Indo Gangetic plain (1000 – 500 hPa) (discussed in section 4).

3.4 Ozone distribution in the anticyclone

Atmos. Chem. Phys. Discuss., doi:10.5194/acp-2016-582, 2016
Manuscript under review for journal Atmos. Chem. Phys.
Published: 20 July 2016

Atmospheric Chemistry and Physics Discussions

We estimate changes in NO_x and ozone in the monsoon anticyclone from Ind38, Ind73 and Chin73 simulations with respect to the CTRL simulation. The distribution of these species is shown at 110 hPa as representative for the anticyclone. Figures 5(a)-(c) depict percentage changes in NO_x mixing ratios for Ind38, Ind73 and Chin73 simulations. A maximum in the NO_x anomalies in the ASM anticyclone (20°E to 120°E) is seen in all the simulations. Ozone anomalies are high at the eastern part of monsoon anticyclone since convective injection into the anticyclone occurs at the eastern part of anticyclone (Fadnavis et al., 2013). Percentage increase in NO_x amounts in the Ind38 simulation is higher (Figure 5(a)) than that in the Ind73 simulation (Figure 5(b)). This is mainly due to descending motion over the central India, as seen in the previous sections. However, the Chin73 simulation shows higher values of increasing NO_x (>18%) in the monsoon anticyclone (Figure 5(c)). In the anticyclone, the increase in ozone mixing ratios in Ind38 simulation is 1-3%, Ind73 is 1-5% and Chin73 is 1-8%. These figures show that easterly jet transport NOx and ozone (from India and China) to Saudi Arabia, Iran and Iraq.

4. Discussion

Increase in ozone mixing ratios may enhance ozone radiative forcing and exert warming (Brasseur, 1997). We estimate anomalies in ozone radiative forcing at the top of the atmosphere for Ind38, Chin73, Ind73 with respect to CTRL simulation over central India (20º-30ºN, 75º-85ºE) and China (30º-45ºN, 100º-135ºE). The increase in ozone radiative forcing over India, in the Ind38 simulation is 0.112 W/m^2, and in the Chin73 simulation is 0.121 W/m^2. In comparison, the estimated global average radiative forcing due to increases in tropospheric ozone since pre-industrial times is estimated to be $+0.35 \pm 0.15$ Wm^{-2} (Brasseur et al., 1997; IPCC, Ramaswamy et al., 2001).

Further, we analyze the temperature anomalies for the Ind38, Ind73 and Chin73 simulations. Figures 6(a)-(c) show the zonal distribution of temperature anomalies. These simulations show surface

Atmos. Chem. Phys. Discuss., doi:10.5194/acp-2016-582, 2016
Manuscript under review for journal Atmos. Chem. Phys.
Published: 20 July 2016

warming over the 30º-40ºN, regions covering North India and North China. The striking feature evident in Ind38, and Chin73 simulations is anomalous warming over the Tibetan Plateau while it is subdued in Ind73 simulation.

In order to understand the atmospheric heating caused due to ozone, we calculate the ozone heating rate using the radiative transfer model, SBDART. ECHAM5-HAMMOZ model simulated temperature, pressure, as well as water vapour concentration and ozone concentrations at various levels are incorporated into the SBDART model in order to estimate the ozone heating rate in the vertical. Figure 7(a) shows the vertical profile of ozone radiative heating rate as obtained from CTRL simulation averaged over Indian (70º-94ºE, 20º-30ºN) and Chinese (70º-100ºE, 30º-40ºN) regions. It shows a high value of ~ 0.003- 0.009 K/day at ~1-4 km. A net radiative heating rate of 0.004 – 0.008 K/day in the troposphere due to changes in ozone was earlier reported by Ramaswamy and Bowen (1994).

Anomalous warming over the Tibetan plateau seen in Figure 6 may be due to heating caused by ozone. Figure 7(b) shows the vertical distribution of anomalies in ozone heating rates averaged over Tibetan plateau (70-100°E, 20-40°N). Positive ozone heating rate anomaly (0.0005-0.0001 K/day) is seen below14 km in Ind38 and Chin73, on the contrary, Ind73 shows negative anomalies in ozone heating rate below 8 km. In the upper troposphere (8 – 14 km) ozone heating rates are positive in all the simulations. They are less in Ind73 ($2.09 \times 10^{-6} – 4.5 \times 10^{-6}$ K/day) as compared to Ind38 ($1.91 \times 10^{-5} – 2.74 \times 10^{-5}$ K/day) and Chin73 (2.17×10^{-5} - 2.99×10^{-5} K/day). The estimated heating rates over the Indo Gangetic plain are ~ 3×10^{-4} K/day (averaged over 1000-800 hPa) this may be due to high amount of ozone production. Ozone heating rate anomaly of $\pm 2 \times 10^{-4}$ K/day was previously reported by Guo et al., 2008, over East Asia and the Tibetan plateau region.

From figures 3, 6 and 7 it can be said that doubling of NO_x emissions (Ind73 simulation) over India increases net ozone production over Indo Gangetic plain. Enhanced ozone production leads to anomalous ozone heating in the lower troposphere over the Indo Gangetic plain (~3×10^{-4} K/day). This

Atmos. Chem. Phys. Discuss., doi:10.5194/acp-2016-582, 2016
Manuscript under review for journal Atmos. Chem. Phys.
Published: 20 July 2016

elicited reversal of monsoon Hadley cell circulation. The descending branch of monsoon Hadley cell circulation over central India (figures 2 and 4) resisted vertical transport of ozone which resulted in subdued Tibetan plateau warming.

The meridional temperature gradient in the upper troposphere over the Tibetan plateau during the monsoon is one of the key factors responsible for the ASM circulation (Flohn 1957; Yanai et al., 1992; Meehl, 1994; Li and Yanai, 1996; Wu and Zhang, 1998). Flohn (1957, 1960) suggested that warming over the Tibetan plateau leads to a reversal of the meridional temperature gradient triggering large-scale change in the general circulation over Asia. The warm ascending air above the Tibetan plateau gradually spreads southward and descends over the northern Indian Ocean. The south-westerly winds at the surface on the other hand complete the Hadley cell. This local circulation system releases latent heat and further maintains the Tibetan high warm core. Thus heating over the Tibetan plateau leads to increased Indian summer monsoon rainfall by enhancing the cross-equatorial circulation and concurrently strengthening both the Somali Jet and the westerly winds that bring rainfall to India (Rajagopalan and Molnar, 2013, Vinoj et al., 2014). Goswami et al., (1999) also reported that there is a strong correlation between Hadley circulation and monsoon precipitation.

Figures 8(a)-(c) depict the monsoon Hadley cell circulation (averaged over 70ºE-110ºE) obtained from the Ind38 Ind73 and Chin73 simulations. The Ind38 and Chin 73 simulations show strengthening of the Hadley circulation; a strong ascending branch of the Hadley cell around 20ºN (Figure 8(a)), whereas it is reversed in Ind73 simulation (Figure 8(b)). Consequently, precipitation anomalies over the Indian region are positive (0.3 – 0.9 mm/day) in Ind38 and Chin73 simulations (figure 8(d)) whereas they are negative in Ind73 simulation (-0.3 – -0.6 mm/day) (Figure 9(e)). Thus enhanced Indian and Chinese NO_x emissions increases warming over the Tibetan plateau by ozone heating and enhances precipitation over India via strengthening Hadley circulation. Whereas doubling

Atmos. Chem. Phys. Discuss., doi:10.5194/acp-2016-582, 2016
Manuscript under review for journal Atmos. Chem. Phys.
Published: 20 July 2016

of NO_x emissions over India produced high amount of ozone over the Indo Gangetic plain. Related ozone heating in the lower troposphere reverses the monsoon Hadley circulation and thereby resulted in negative precipitation anomalies.

5. Conclusions

In this paper we investigate the potential impacts of enhanced anthropogenic NO_x emissions on ozone production and distribution during the monsoon season using the state-of-the-art ECHAM5-HAMMOZ model simulations. We performed sensitivity experiments for anthropogenic NO_x enhancement, 38% over India (Ind38 simulation) and 73% over China (Chin73 simulation) in accordance with observed trends 3.8% per year over India and 7.3% per year over China (Ghude et al., 2013; Schneider and van der A, 2012). In another experiment, anthropogenic NO_x emissions over India are doubled (73%), equal to China (Ind73 simulation).

These simulations show that increase in anthropogenic NO_x emissions (over India and China) increases ozone production in the lower and mid-troposphere. The monsoon convection at the southern flank of the Himalayas (80-90°E) and over the Bay of Bengal lifts up the NO_x and ozone from India across tropopause into the lower stratosphere. Cross tropopause transport also occurs over China due to convection over the South China Sea. These air masses are then transported deeper into the stratosphere via the tropical pipe.

Increase in NO_x emissions in Ind38 and Chin73 simulations increases ozone radiative forcing over India by 0.112 W/m^2 and 0.121 W/m^2 respectively. Enhanced ozone production (Ind38 and Chin73 simulations) increases ozone heating rates which cause anomalous warming over the Tibetan plateau. Doubling of NO_x emissions over the India region (Ind73 simulation) produces anomalous heating near surface over the Indo Gangetic plain (~3×10^{-4} K/day) due to high amount of ozone

Atmos. Chem. Phys. Discuss., doi:10.5194/acp-2016-582, 2016
Manuscript under review for journal Atmos. Chem. Phys.
Published: 20 July 2016

Atmospheric Chemistry and Physics Discussions

production (~40-90%). This elicited subsidence over central India (via reversal of monsoon Hadley circulation) and resisted vertical transport of ozone which resulted in subdued Tibetan plateau warming.

In Ind38 and Chin73 simulations, anomalous warming over the Tibetan plateau resulted in strengthening of the monsoon Hadley circulation over India and elicited positive precipitation (0.3 – 0.9 mm/day) anomalies over India. However, doubling of NO_x emissions over India (Ind73) induced reverse Hadley circulation due to anomalous heating, in the lower troposphere over the Indo Gangetic plain. The descending branch of the Hadley circulation resisted the cross tropopause transport of ozone and NO_x. The reversal of the Hadley circulation and concurrent subdued warming over the Tibetan plateau resulted in negative precipitation anomalies (-0.3 – -0.6 mm/day) over India.

Atmos. Chem. Phys. Discuss., doi:10.5194/acp-2016-582, 2016
Manuscript under review for journal Atmos. Chem. Phys.
Published: 20 July 2016

Atmospheric Chemistry and Physics Discussions

References:

Bian, J., Pan, L. L., Paulik, L., Vömel, H., Chen, H., and Lu, D.: In situ water vapor and ozone measure-ments in Lhasa and Kunming during the Asian summer monsoon, Geophys. Res. Lett., 39, L19808, doi:10.1029/2012GL052996, 2012.

Braesicke, P., Smith, O. J., Telford, P., & Pyle, J. A.: Ozone concentration changes in the Asian summer monsoon anticyclone and lower stratospheric water vapour: An idealised model study. Geophysical Research Letters, 38(3), doi: 10.1029/2010GL046228, 2011.

Brasseur, G.P., Kiehl, J.T., Müller, J.F., Schneider, T., Granier, C., Tie, X. and Hauglustaine, D.: Past and future changes in global tropospheric ozone: Impact on radiative forcing. Geophys. Res. Lett., 25(20), 3807-3810, doi: 10.1029/1998GL900013,1998.

Brasseur, Guy P., Edited. The stratosphere and its role in the Climate System. Vol. 54. Springer Science & Business Media, 2013.

Chen, B., Xu, X., D, Yang, S., and Zhao, T. L.: Climatological perspectives of air transport from atmospheric boundary layer to tropopause layer over Asian monsoon regions during boreal summer inferred from Lagrangian approach, Atmos. Chem. Phys., 12, 5827–5839, doi:10.5194/acp-12-5827-2012. 2012.

Derwent, R. G.: Trace Gases and their Relative Contribution to the Greenhouse Effect, AERE Report R-13716, H.M. Stationery Office, London. 1990.

Dunkerton, T. J.: Evidence of meridional motion in the summer lower stratosphere adjacent to monsoon regions, J. Geophys. Res., 100, 16,675–16,688, doi: 10.1029/95JD01263, 1995.

Elampari, K., Chithambarathanu, T., Krishna Sharma, R., and Johnson Jeyakumar, S.: Surface ozone air pollution in Nagercoil, India, Indian Journal of Science and Technology, 4(3), 181-184, doi: 10.17485/ijst/2011/v4i3/29961, 2011.

Fadnavis, S., Semeniuk, K., Pozzoli, L., Schultz, M. G., Ghude, S. D., Das, S., and Kakatkar, R.: Transport of aerosols into the UTLS and their impact on the Asian monsoon region as seen in a global model simulation, Atmos. Chem. Phys., 13, 8771–8786, doi:10.5194/acp-13-8771-2013, 2013.

Fadnavis, S., Semeniuk, K., Schultz, M. G., Mahajan, A., Pozzoli, L., Sonbawane, S., and Kiefer, M.: Transport pathways of peroxyacetyl nitrate in the upper troposphere and lower stratosphere from different monsoon systems during the summer monsoon season, Atmos. Chem. Phys. Discuss., 14, 20159–20195, doi:10.5194/acpd-14-20159-2014, 2014.

Fadnavis, S., Semeniuk, K., Schultz, M. G., Kiefer, M., Mahajan, A., Pozzoli, L., and Sonbawane, S.: Transport pathways of peroxyacetyl nitrate in the upper troposphere and lower stratosphere from different monsoon systems during the summer monsoon season. Atmos. Chem. and Phys., 15, doi:10.5194/acp-15-11477-2015, 11477-11499, 2015.

Fiore, A. M., Horowitz, L. W., Purves, D. W., Levy II, H., Evans, M. J., Wang, Y., Li, Q., and Yantosca, R. M.: Evaluating the contribution of changes in isoprene emissions to surface ozone trends over the eastern United States, J. Geophys. Res., 110, D12303, doi:10.1029/2004JD005485, 2005.

Flohn, H.: Large-scale aspects of the summer monsoon in South and East Asia, J. Meteor. Soc. Japan, 75, 180–186, doi: 551.553.21:551.589.5, 1957.

Flohn, H.: Recent investigations on the mechanism of the “Summer Monsoon” of Southern and Eastern Asia, Proc. Symp. Monsoon of the World, 1960.

Forster, F., Piers, M., and Keith, P. Shine: Radiative forcing and temperature trends from stratospheric ozone changes, J. Geophys Res, 102, 10841-10855, 1997.

Froidevaux, L., Livesey, N. J., Read, W. G., Jiang, Y. B., Jimenez, C. J., Filipiak, M. J., Schwartz, M. J., Santee, M. L., Pumphrey, H. C., Jiang, J. H., Wu, D. L., Manney, G. L., Drouin, B. J.,

Waters, J. W., Fetzer, E. J., Bernath, P. F., Boone, C. D., Walker, K. A., Jucks, K. W., Toon, G. C., Margitan, J. J., Sen, B., Webster, C. R., Christensen, L. E., Elkins, J. W., Atlas, E., Ueb, R. A., and Hendershot, R.: Early validation analyses of atmospheric profiles from EOS MLS on the Aura satellite. IEEE Trans. Geosci. Remote Sensing 44, 1106 – 1121, doi: 10.1109/TGRS.2006.864366, 2006.

Fu, R., Hu, Y. L., Wright, J. S., Jiang, J. H., Dickinson, R.E., Chen, M. X., Filipiak, M., Read, W. G., Waters, J. W.,and Wu, D. L.: Short circuit of water vapor and polluted air to the global stratosphere by convective transport over the Tibetan Plateau, P. Natl. Acad. Sci. USA, 103, 5664–5669, doi:10.1073/pnas.0601584103, 2006.

Fujita, E. M., Croes, B. E., Bennett, C. L., Lawson, D. R., Lurmann, F. W., and Main, H. H.: Comparison of emission inventory and ambient concentration ratios of CO, NMOG, and NOx in California's South Coast Air Basin. Journal of the Air & Waste Management Association, 42(3), 264-276, doi: 10.1080/10473289.1992.10466989, 1992.

Ganzeveld, L. and Lelieveld, J.: Dry deposition parameterization in a chemistry general circulation model and its influence on the distribution of reactive trace gases, J. Geophys. Res., 100, 20999–21012, doi:10.1029/95JD02266, 1995.

Garny, H. and Randel, W. J.: Dynamic variability of the Asian monsoon anticyclone observed in potential vorticity and correlations with tracer distributions, J. Geophys. Res. Atmos., 118, 13,421–13,433, doi:10.1002/2013JD020908, 2013.

Gettelman, A., Kinnison, D. E., Dunkerton, T. J., and Brasseur, G. P.: Impact of monsoon circulations on the upper troposphere and lower stratosphere, J. Geophys. Res., 109, D22101, doi:10.1029/2004jd004878, 2004.

Ghude, S. D., Kulkarni, S. H., Jena, C., Pfister, G. G., Beig, G., Fadnavis, S., and van der A R. J.: Application of satellite observations for identifying regions of dominant sources of nitrogen oxides over the Indian Subcontinent, J. Geophys. Res., 118, 1–15, doi:10.1029/2012JD017811, 2013.

Goswami, B. N., Krishnamurthy, V., and Annamalai, H.: A broad-scale circulation index for the interannual variability of the Indian summer monsoon. Q. J. R. Meteorol. soc., 125, 611-633, doi: 10.1002/qj.49712555412, 1999.

Gu, D., Wang, Y., Smeltzer, C., and Boersma, K. F.: Anthropogenic emissions of NOx over China: Reconciling the difference of inverse modeling results using GOME-2 and OMI measurements, J. Geophys. Res. Atmos., 119, doi:10.1002/ 2014JD021644, 2014.

Guo, W. W., Yuan, M., Wang, H. Y., Sun, J. H., Xie, Y. Q., Fan, W. X., and Chen, X. M.: A Study of Ozone Amount in the Transition Layer Between Troposphere and Stratosphere and Its Heating Rate, Chinese Journal of Geophysics, 51(5), 916-930, 2008.

Hilboll, A., Richter, A., and Burrows, J. P.: Long-term changes of tropospheric NO2 over megacities derived from multiple satellite instruments, Atmos. Chem. Phys., 13, 4145–4169, doi:10.5194/acp-13-4145-2013, 2013.

Horowitz, L. W., Walters, S., Mauzerall, D. L., Emmons, L. K., Rasch, P. J., Granier, C., Tie, X., Lamarque, J., Schultz, M. G.,Tyndall, G. S., Orlando, J. J., and Brasseur, G. P.: A global simulation of tropospheric ozone and related tracers, Description and evaluation of MOZART, version 2, J. Geophys. Res., 108, 4784, doi:10.1029/2002JD002853, 2003.

Jacob, D. J., Logan, J. A., and Murti, P. P.: Effect of rising Asian emissions on surface ozone in the United States, Geophys. Res. Lett., 26, 2175–2178, doi:10.1029/1999GL900450, 1999.

Konopka, P., Grooß, J.U., Günther, G., Ploeger, F., Pommrich, R., Müller, R. and Livesey, N.: Annual cycle of ozone at and above the tropical tropopause: observations versus simulations with the Chemical Lagrangian Model of the Stratosphere (CLaMS), Atmos. Chem. Phys., 10(1), 121-132, doi: www.atmos-chem-phys.net/10/121/2010/, 2010.

Kunze, M., Braesicke, P., Langematz, U., Stiller, G., Bekki, S., Brühl, C., Chipperfield, M., Dameris, M., Garcia, R. and Giorgetta, M.: Influences of the Indian summer monsoon on water vapor and ozone concentrations in the UTLS as simulated by chemistry-climate models, J Clim, 23(13), 3525-3544, doi: http://dx.doi.org/10.1175/2010JCLI3280.1, 2010.

Lacis Andrew, A., Donald Wuebbles, J., and Jennifer Logan A., Radiative Forcing of climate by Changes in the Vertical Distribution of Ozone, J. Geophys. Res., 95 , 9971-9981, doi: 10.1029/JD095iD07p09971, 1990.

Lawrence, M. G.: Atmospheric science: Asia under a high-level brown cloud, Nat. Geosci., 4, 352–353, doi:10.1038/ngeo1166, 2011.

Lee, Y. C., Shindell, D. T., Faluvegi, G., Wenig, M., Lam, Y. F., Ning, Z., Hao, S., and Lai, C. S.: Increase of Ozone concentrations, Its Temperature Sensitivity And The Precursor Factor In South China, Tellus B, 66, 23455, doi: http://Dx.Doi.Org/10.3402/Tellusb.V66.23455, 2014.

Lei, W., Zhang, R., Tie, X., and Hess, P.: Chemical characterization of ozone formation in the Houston-Galveston area. J.Geophys.Res., 109, doi: 10.1029/2003JD004219, 2004.

Li, C. and Yanai M.: The onset and interannual variability of the Asian summer monsoon in relation to land–sea thermal contrast, J. Clim. 9: 358–375, doi: http://dx.doi.org/10.1175/1520-0442(1996)009<0358:TOAIVO>2.0.CO;2, 1996.

Li, Q., Jiang, J. H., Wu, D. L., Read, W. G., Livesey, N. J., Waters, J. W., Zhang, Y., Wang, B.,. Filipiak, M. J, Davis, C. P., Turquety, S., Wu, S., Park, R. J., Yantosca, R. M., and Jacob, D. J.: Convective outflow of south Asian pollution: a global CTM simulation compared with EOS MLS observations, Geophys. Res. Lett., 32, doi: http://dx.doi.org/10.1029/2005GL022762, doi: 10.1029/2005GL022762, 2005.

Livesey, N. J., Read, W. G., Froideveaux, L., Lambert, A., Manney, G. L., Pumphrey, H. C., Santee, M. L., Schwartz, M. J., Wang, S., Cofield, R. E., Cuddy, D. T., Fuller, R. A., Jarnot, R. F., Jiang, J. H., Knosp, B. W., Stek, P. C., Wagner, P. A., and Wu, D. L.: Version 3.3 Level 2 data quality and description document. Tech Rep. JPL D-33509, Jet Propulsion Laboratory, available at: http://mls.jpl.nasa.gov (last access: 17 August 2015), 2011.

Livesey, N. J., Read, W. G., Filipiak, M. J., Froidevaux, L., Harwood, R. S., Jiang, J. H., Jimenez, C., Pickett, H. M., Pumphrey, H. C., Santee, M. L., Schwartz, M. J., Waters, J. W., and Wu, D. L.: EOS MLS Version 1.5 Level 2 data quality and description document, JPL, California, 2005.

Meehl, G. A.: Coupled land-ocean-atmosphere processes and South Asian monsoon variability, Science, 266, 263–267, doi: 10.1126/science.266.5183.263, 1994.

Park, M., Randel, W. J., Gettelman, A., Massie, S. T., and Jiang, J.H.: Transport above the Asian summer monsoon anticyclone inferred from Aura Microwave Limb Sounder tracers, J. Geophys.Res., 112, D16309,doi:10.1029/2006jd008294, 2007.

Park, M., Randel, W. J., Emmons, L. K., and Livesey, N. J.:Transport pathways of carbon monoxide in the Asian summer monsoon diagnosed from Model of Ozone and Related Tracers (MOZART), J. Geophys. Res., 114, D08303, doi:10.1029/2008jd010621, 2009.

Penki, R. K. and Kamra, A. K.: Lightning distribution with respect to the monsoon trough position during the Indian summer monsoon season, J. Geophy. Res., 118, 4780–4787, doi:10.1002/jgrd.50382, 2013.

Pozzoli, L., Bey, I., Rast, J. S., Schultz, M. G., Stier, P., and Feichter, J.: Trace gas and aerosol interactions in the fully coupled model of aerosol-chemistry-climate ECHAM5- HAMMOZ: 1. Model description and insights from the spring 2001 TRACE-P experiment, J. Geophys. Res., 113, D07308, doi:10.1029/2007JD009007, 2008a.

Pozzoli, L., Bey, I., Rast, J. S., Schultz, M. G., Stier, P., and Feichter, J.: Trace gas and aerosol interactions in the fully coupled model of aerosol-chemistry-climate ECHAM5- HAMMOZ: 2. Impact of heterogeneous chemistry on the global aerosol distributions, J. Geophys. Res., 113,

D07309, doi:10.1029/2007JD009008, 2008b.
Pozzoli, L., Janssens-Maenhout, G., Diehl, T., Bey, I., Schultz, M. G., Feichter, J., Vignati, E., and Dentener, F.: Re-analysis of tropospheric sulfate aerosol and ozone for the period 1980–2005 using the aerosol-chemistry-climate model ECHAM5-HAMMOZ, Atmos. Chem. Phys., 11, 9563–9594, doi:10.5194/acp-11-9563-2011, 2011.
Rajagopalan, B., and Molnar, P.: Signatures of Tibetan Plateau heating on Indian summer monsoon rainfall variability, J. Geophys. Res. Atmos., 118, 1170–1178, doi:10.1002/jgrd.50124, 2013.
Ramanathan, V., Callis, L., Cess, R., Hansen, J., Isaksen, I., Kuhn, W., Lacis, A., Luther, F., Mahlman, J., Reck, R., and Schlesinger, M.: Climate-Chemical Interactions and Effects of Changing Atmospheric Trace Gases, Rev. Geophys. 25, 1441–1482, doi: 10.1029/RG025i007p01441, 1987.
Ramaswamy, V. and Bowen, M.M.: Effect of changes in radiatively active species upon the lower stratospheric temperatures, Journal Of Geophysical Research-All Series-, 99, 18-909, doi: 0418-0227/94/94JD-01310$05.00, 1994.
Ramaswamy, V., Boucher, O., Haigh, J., Hauglustaine, D., Haywood, J., Myhre, G., Nakajima, T., Shi, G. Y., and Solomon, S.: Radiative Forcing of Climate Change, Chapter 6, in: Climate Change 2001, The scientific basis: Contribution of working group I to the Third assessment report of the Intergovernmental Panel on Climate, edited by: Houghton, J. T., Ding, Y., Griggs, Y., Noguer, M., v.d. Linden, P. J., Dai, X., Maskell, K., and Johnson, C. A., pp. 881, Cambridge University Press, Cambridge, United Kingdom and New York, NY, US, doi: 10.1256/004316502320517344, 2001.
Ranalkar, M. R. and Chaudhari, H. S.: Seasonal variation of lightning activity over the Indian subcontinent, Meteorol. Atmos.Phys., 104, 125–134, doi: 10.1007/s00703-009-0026-7, 2009.
Randel, W. J., Wu, F., Gettelman, A., Russell, J. M., Jawodny, J. M., and Oltmans, S. J.: Seasonal variation of water vapor in the lower stratosphere observed in Halogen Occultation Experiment data, J. Geo-phys. Res., 106, 14,313 – 14,325, doi: 0148-0227/01/2001JD900048509.00, 2001.
Randel, W. J., and Park M.: Deep convective influence on the Asian summer monsoon anticyclone and associated tracer variability observed with Atmospheric Infrared Sounder (AIRS), J. Geophys. Res.,111, D12314, doi:10.1029/2005JD006490, 2006.
Randel, W. J., Park, M., Emmons, L., Kinnison, D., Bernath, P., Kaley Walker, A., Boone, C., and Pumphrey, H.: Asian Monsoon Transport of Pollution to the Stratosphere Science, 328(5978), 611-613, doi: 10.1126/science.1182274, 2010.
Ricchiazzi, P., Yang, S., Gautier, C., and Sowle, D.: SBDART, A research and teaching tool for plane-parallel radiative transfer in the Earth's atmosphere, Bull. Am. Meteorol. Soc., 79, 2101–2114. 1998.
Richter, A., John Burrows, P., Hendrik, N., Granier C., and Niemeier, U.: Increase in tropospheric nitrogen dioxide over China observed from space; 437, doi:10.1038/nature04092, 2005.
Riese, M., Ploeger, F., Rap, A., Vogel, B., Konopka, P., Dameris, M. and Forster, P.: Impact of uncertainties in atmospheric mixing on simulated UTLS composition and related radiative effects, J. Geophys. Res.: Atmos., 117(D16), doi: 10.1029/2012JD017751, 2012.
Roeckner, E., Bauml, G., Bonaventura, L., Brokopf, R., Esch, M., Giorgetta, M., Hagemann, S., Kirchner, I., Kornblueh, L., Manzini, E., Rhodin, A., Schlese, U., Schulzweida, U., and Tompkins, A.: The atmospehric general circulation model ECHAM5: Part 1, Tech. Rep. 349, Max Planck Institute for Meteorology,Hamburg, 2003.
Roldugin, V., and Henriksen, K.: Horizontal movements in the ozone layer, accepted for publication in, J. Atm. terr. Phys , 1995.
Sander, S. P., Fried, R. R., Barker, J. R., Golden, D. M., Kurylo, M. J.,Wine, P. H., J. Abbatt, P. D., 25 Burkholder, J. B., Kolb, C. E., Moortgat, G. K., Huie, R. E., and Orkin, V. L.: Chemical

kinetics and photochemical data for use in atmospheric studies, evaluation number 14, JPL Publ. 02-25, Jet Propul. Lab., Calif. Inst. Of Technol., Pasadena, available at: http://jpldataeval.jpl.nasa.gov/pdf/JPL_02-25_rev02.pdf, 2003.

Schneider, P. and van der A. R. J.: A global single-sensor analysis of 2002–2011 tropospheric nitrogen dioxide trends observed from space, J, Geophy. Res., 117, D16309, doi:10.1029/2012JD017571, 2012.

Schoeberl, M. R., Duncan, B. N., Douglass, A. R., Waters, J., Livesey, N., Read, W., and Filipiak, M.: The carbon monoxide tape recorder. Geophys. Res. Lett., 33(12), doi: 10.1029/2006GL026178, 2006.

Sillman, S.: The use of NOy, H_2O_2, and HNO_3 as indicators for ozone-NO_x-hydrocarbon sensitivity in urban locations. J. Geophys. Res., 100, 14,175–14,188, doi: 10.1029/94JD02953, 1995.

Sinha, V., Kumar, V., and Sarkar, C.: Chemical composition of pre-monsoon air in the Indo-Gangetic Plain measured using a new air quality facility and PTR-MS: high surface ozone and strong influence of biomass burning, Atmos. Chem. Phys., 14, 5921–5941, 2014. doi:10.5194/acp-14-5921-2014, 2014.

Søvde, O. A., Hoyle, C. R., Myhre, G., and Isaksen, I. S. A.: The HNO3 forming branch of the HO2 + NO reaction: pre-industrial-to-present trends in atmospheric species and radiative forcings, Atmos. Chem. Phys., 11, 8929–8943, 2011; doi:10.5194/acp-11-8929-2011, 2011.

Stevenson, D. S., P. J. Young, Vaishali, N., Lamarque, J. F., Drew, T., Shindell, Voulgarakis, A., and Skeie R. B.: Tropospheric ozone changes, radiative forcing and attribution to emissions in the Atmospheric Chemistry and Climate Model Intercomparison Project (ACCMIP), Atmos. Chem. Phys., 13, 3063-3085, doi:10.5194/acp-13-3063-2013, 2013.

Stier, P., Feichter, J., Kinne, S., Kloster, S., Vignati, E., Wilson, J., Ganzeveld, L., Tegen, I., Werner, M., Balkanski, Y., Schulz, M., Boucher, O., Minikin, A., and Petzold, A.: The aerosol-climate model ECHAM5-HAM, Atmos. Chem. Phys., 5, 1125–1156, doi:10.5194/acp-5-1125-2005, 2005.

Thuburn, J. and Craig, G.C.: On the temperature structure of the tropical substratosphere, Journal of Geophysical Research: Atmospheres, 107(D2), doi: 10.1029/2001JD000448, 2002.

Tie, X. X., Zhang, R., Brasseur, G., Emmons, L., and Lei, W.:Effects of lightning on reactive nitrogen and nitrogen reservoir species in the troposphere, J. Geophys. Res.-Atmos., 106, 3167– 3178, doi:10.1029/2000JD900565, 2001.

Tie, X., Madronich, S., Li, G.H., Ying, Z.M., Zhang, R., Garcia, A., Lee-Taylor, and J., Y. Liu. Characterizations of chemical oxidants in Mexico City: a regional chemical/dynamical model (WRF-Chem) study, Atmos. Environ., 41, 1989–2008, doi:10.1016/j.atmosenv.2006.10.053, 2007.

Tobo, Y., Iwasaka, Y., Zhang, D., Shi, G., Kim, Y. S., Tamura, K., and Ohashi, T.: Summertime ‘‘ozone valley’’ over the Tibetan Plateau derived from ozonesondes and EP/TOMS data, Geophys. Res. Lett., 35, L16801, doi:10.1029/2008GL03434, 2008.

Vernier, J.-P., T. D. Fairlie, M. Natarajan, F. G. Wienhold, J. Bian, B. G. Martinsson, S. Crumeyrolle, L. W. Thomason, and Bedka, K.: Increase in upper tropospheric and lower stratospheric aerosol levels and its potential connection with Asian Pollution, J. Geophys. Res. Atmos., 120, 1608–1619, doi:10.1002/2014JD022372, 2015.

Vinoj, V., Rasch, P.J., Wang, H., Yoon, J.H., Ma, P.L., Landu, K. and Singh, B.: Short-term modulation of Indian summer monsoon rainfall by West Asian dust, Nature Geoscience, *7*(4), 308-313, doi:10.1038/ngeo2107, 2014.

Vogel B., Günther G., Müller R., Grooß, and Riese M.: Impact of different Asian source regions on the composition of the Asian J.-U. monsoon anticyclone and of the extratropical lowermost stratosphere, Atmos. Chem. Phys., 15, 13699–13716, doi:10.5194/acp-15-13699-2015, 2015.

593 Wang, Y. X., McElroy, M. B., Martin, R.V., Streets, D. G., Zhang, Q., and Fu, T. M.: Seasonal
594 variability of NOx emissions over east China constrained by satellite observations:
595 Implications for combustion and microbial sources, J. Geophys. Res., 112, D06301,
596 doi:10.1029/2006jd007538, 2007.
597 Waters, J. W., Froidevaux, L., Harwood, R.S., Jarnot, R.F., Pickett, H. M., Read, W. G., Siegel, P. H.,
598 Cofield, R. E., Filipiak, M. J., Flower, D. A., Holden, J. R., Lau, G. K., Livesey, N. J., Manney,
599 G. L., Pumphrey, H. C., Santee, M. L., Wu, D. L., Cuddy, D. T., Lay, R. R., Loo, M. S., Perun,
600 V. S., Schwartz, M. J., Stek, P. C., Thurstans, R. P., Boyles, M. A., Chandra, S., Chavez, M. C.,
601 Chen, G. S., Chudasama, B. V., Dodge, R., Fuller, R. A., Girard, M.A., Jiang, J. H., Jiang, Y.,
602 Knosp, B. W., LaBelle, R. C., Lee, K. A., Miller, D., Oswald, J. E., Patel, N. C., Pukala, D.
603 M., Quintero, O., Scaff, D. M., Snyder, W. V., Tope, M. C., Wagner, P. A., and Walch, M. J.:
604 The Earth Observing System Microwave LimbSounder (EOS MLS) on the Aura satellite.IEEE
605 Trans, Geosci.Remote Sensing44, 1075 – 1092, doi: 10.1109/TGRS.2006.873771, 2006.
606 Wild, O., and Akimoto, H.: Intercontinental transport of ozone and its precursors in a three-
607 dimensional global CTM, Jour. Geophys. Res.: Atmos., 106(D21), 27729-27744, doi:
608 http://dx.doi.org/10.1029/2000JD000123, 2001.
609 Wu, G. X., and Zhang, Y. S.: Tibetan Plateau forcing and the timing of the monsoon onset over South
610 Asia and the South ChinaSea, Mon Wea Rev 126:913–927, doi:
611 http://dx.doi.org/10.1175/1520-0493(1998)126<0913:TPFATT>2.0.CO;2, 1998.
612 Yamaji, K., Ohara, T., Uno, I., Tanimoto, H., Kurokawa, J., and Akimoto, H.: Analysis of the seasonal
613 variation of ozone in the boundary layer in East Asia using the Community Multiscale Air
614 Quality model: what controls surface ozone levels over Japan?, Atmos. Environ., 40, 1856–
615 1868, 2006.
616 Yanai, M., Li, C., Song, Z.: Seasonal heating of the Tibetan Plateau and its effects on the evolution of
617 the Asian summer monsoon, J Meteor Soc Japan, 70, 189–221, 1992.
618 Zhang, R.W., Lei, X., and TieHess, P.: Industrial emissions cause extreme diurnal urban ozone
619 variability. Proc. Natl. Acad. Sci. USA, 101, 6346–6350, doi: 10.1073/pnas.0401484101, 2004.
620 Zhao, C. and Wang, Y. H.: Assimilated inversion of NOx emissions over East Asia using OMI NO2
621 column measurements, Geophys.Res. Lett., 36, L06805, doi:10.1029/2008gl037123, 2009.
622 Zhao, B., Wang, S. X., Liu, H., Xu, J. Y., Fu, K., Klimont, Z., Hao, J. M., He, K. B., Cofala, J., and
623 Amann, M.: NOx emissions in China: historical trends and future perspectives, Atmos. Chem.
624 Phys., 13, 9869–9897, doi:10.5194/acp-13-9869-2013, 2013.
625
626

Atmos. Chem. Phys. Discuss., doi:10.5194/acp-2016-582, 2016
Manuscript under review for journal Atmos. Chem. Phys.
Published: 20 July 2016

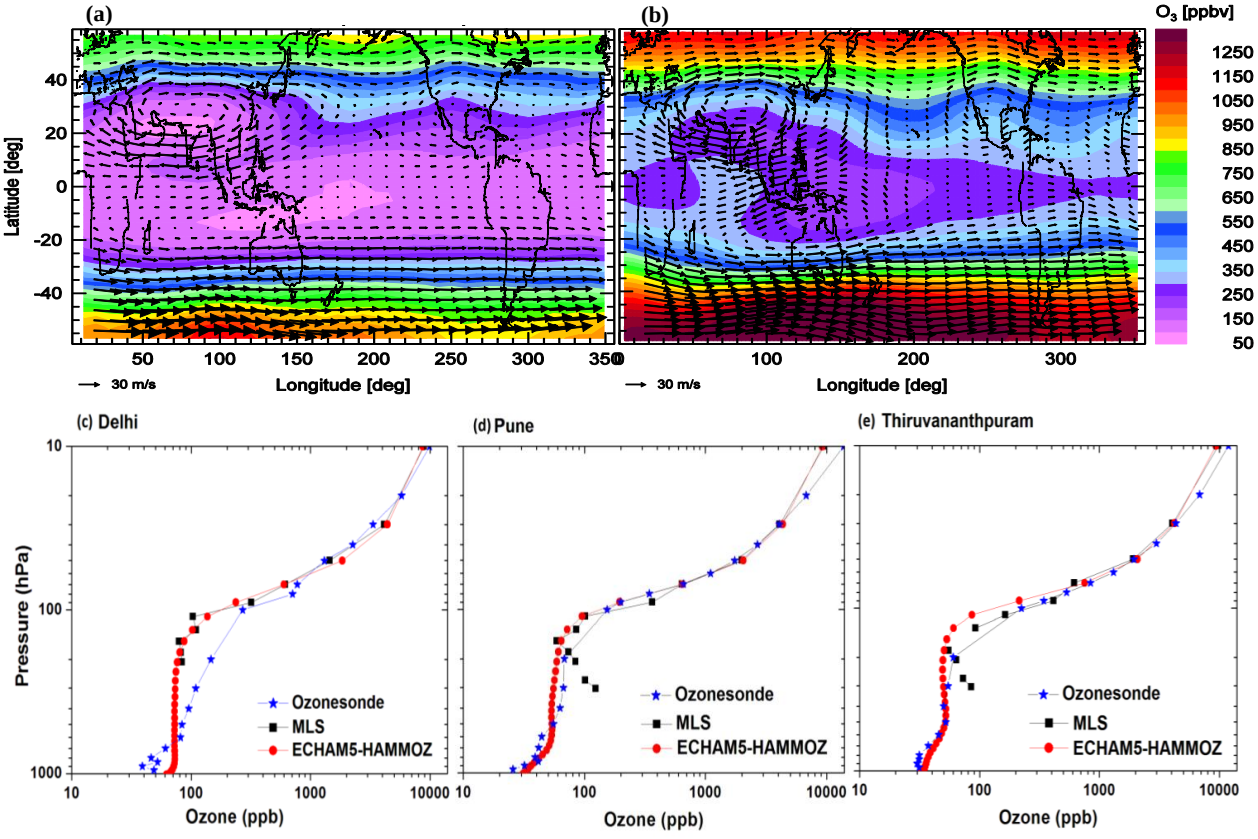

Figure 1: Distribution of ozone mixing ratio (ppbv) during the monsoon season (June-September) obtained from (a) MLS observations at 100 hPa. Black arrows indicate wind vectors from ERA-Interim. Show the same but obtained from (b) ECHAM5-HAMMOZ CTRL simulation at 90 hPa. Black arrows indicate simulated wind vectors. ECHAM5-HAMMOZ simulation is smoothed with averaging kernel of MLS. Vertical distribution of seasonal mean (June-September) ozone mixing ratios (ppb) as obtained from ozonesonde (2001-2009), MLS (2004-2013) and ECHAM5-HAMMOZ CTRL simulation at Indian stations, (c) Delhi (d) Pune (e) Thiruvananthpuram.

Atmos. Chem. Phys. Discuss., doi:10.5194/acp-2016-582, 2016
Manuscript under review for journal Atmos. Chem. Phys.
Published: 20 July 2016

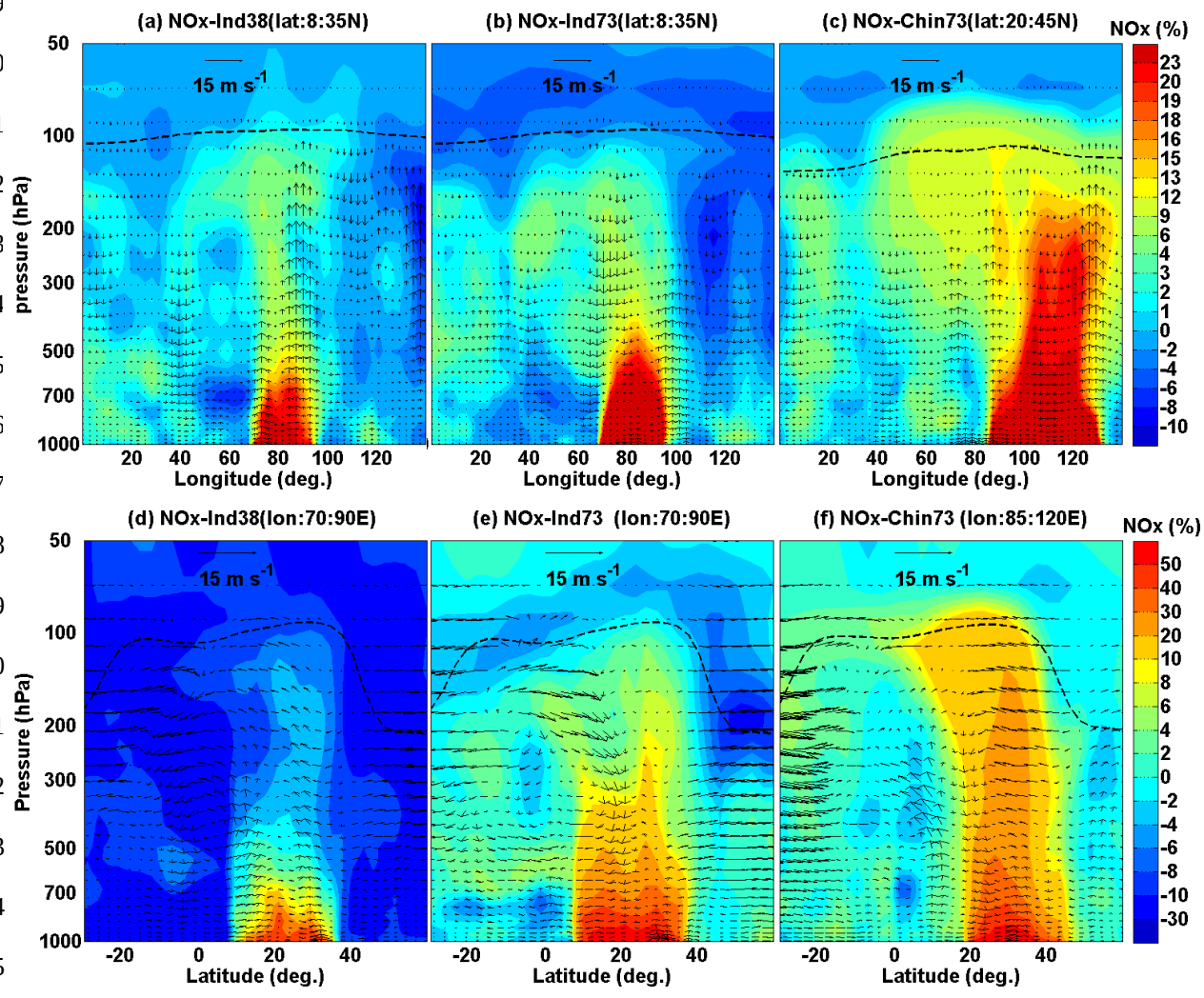

Figure 2: Longitude pressure cross-section of NO_x anomalies (%) averaged for the monsoon season (June-September) obtained from (a) Ind38 (averaged over 8ºN-35ºN), (b) Ind73 (averaged over 8ºN-35ºN), (c) Chin73 (averaged over 20ºN-45ºN) simulations. Latitude pressure cross-section of NO_x anomalies (%) averaged for the monsoon season (June-September) obtained from (d) Ind38 (averaged over 70ºE-90ºE), (e) Ind73 (averaged over 70ºE-90ºE), (f) Chin73 (averaged over 85ºE-120ºE) simulations. Black arrows indicate wind vectors. The vertical velocity field has been scaled by 300. The dashed line represents the tropopause.

Atmos. Chem. Phys. Discuss., doi:10.5194/acp-2016-582, 2016
Manuscript under review for journal Atmos. Chem. Phys.
Published: 20 July 2016

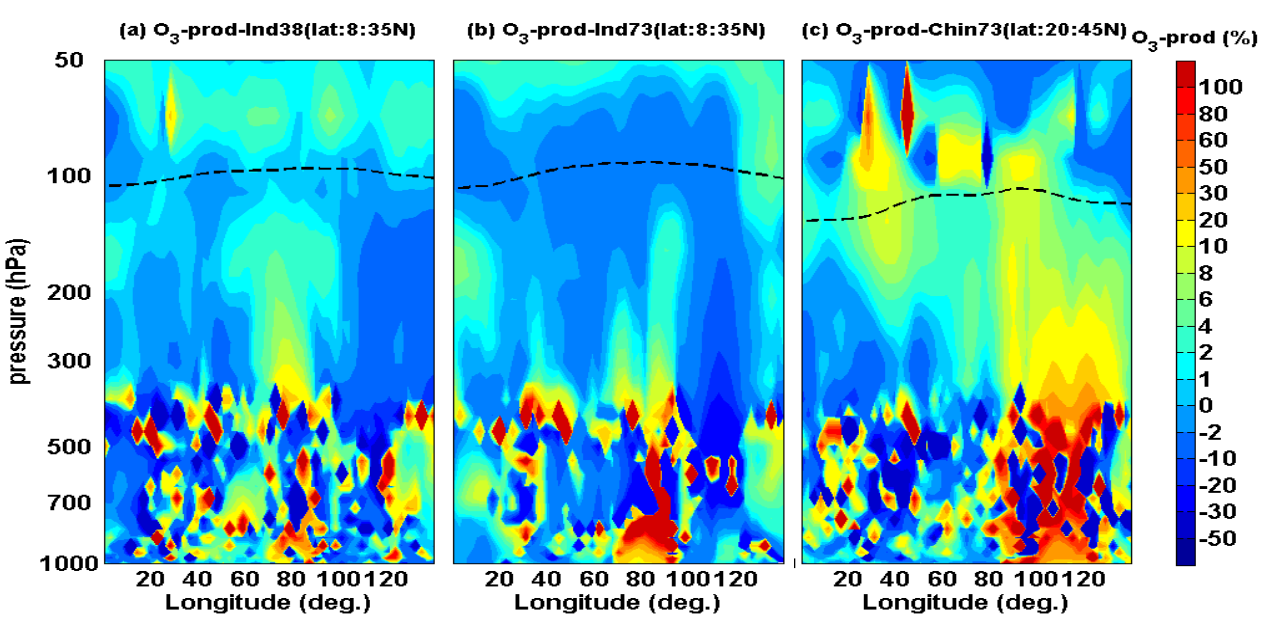

Figure 3: Longitude pressure cross-section of changes in net ozone production (%) (due to enhanced NO_x with respect to CTRL simulation) averaged for the monsoon season (June-September) obtained from (a) Ind38 (averaged over 8ºN-35ºN), (b) Ind73 (averaged over 8ºN-35ºN), (c) Chin73 (over 20ºN-45ºN) simulations. The dashed line represents the tropopause.

Atmos. Chem. Phys. Discuss., doi:10.5194/acp-2016-582, 2016
Manuscript under review for journal Atmos. Chem. Phys.
Published: 20 July 2016

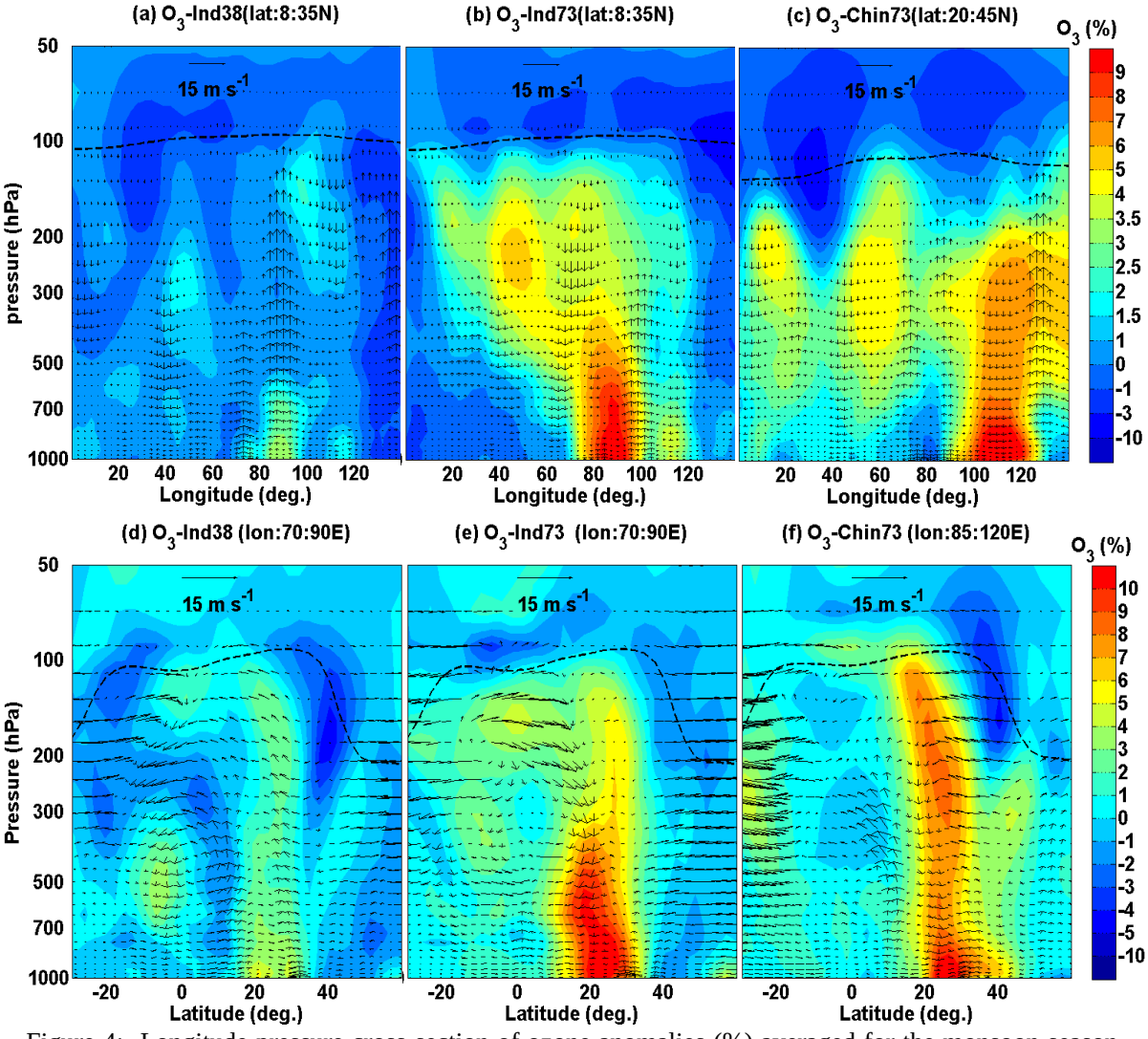

Figure 4: Longitude pressure cross-section of ozone anomalies (%) averaged for the monsoon season (June-September) obtained from (a) Ind38 (averaged over 8ºN-35ºN), (b) Ind73 (averaged over 8ºN-35ºN), (c) Chin73 (averaged over 20ºN-45ºN) simulations. Latitude pressure cross-section of ozone anomalies (%) averaged for the monsoon season (June-September) obtained from (d) Ind38 (averaged over 70ºE-90ºE), (e) Ind73 (averaged over 70ºE-90ºE), (f) Chin73 (averaged over 85ºE-120ºE) simulations. Black arrows indicate wind vectors. The vertical velocity field has been scaled by 300. The dashed line represents the tropopause.

Atmos. Chem. Phys. Discuss., doi:10.5194/acp-2016-582, 2016
Manuscript under review for journal Atmos. Chem. Phys.
Published: 20 July 2016

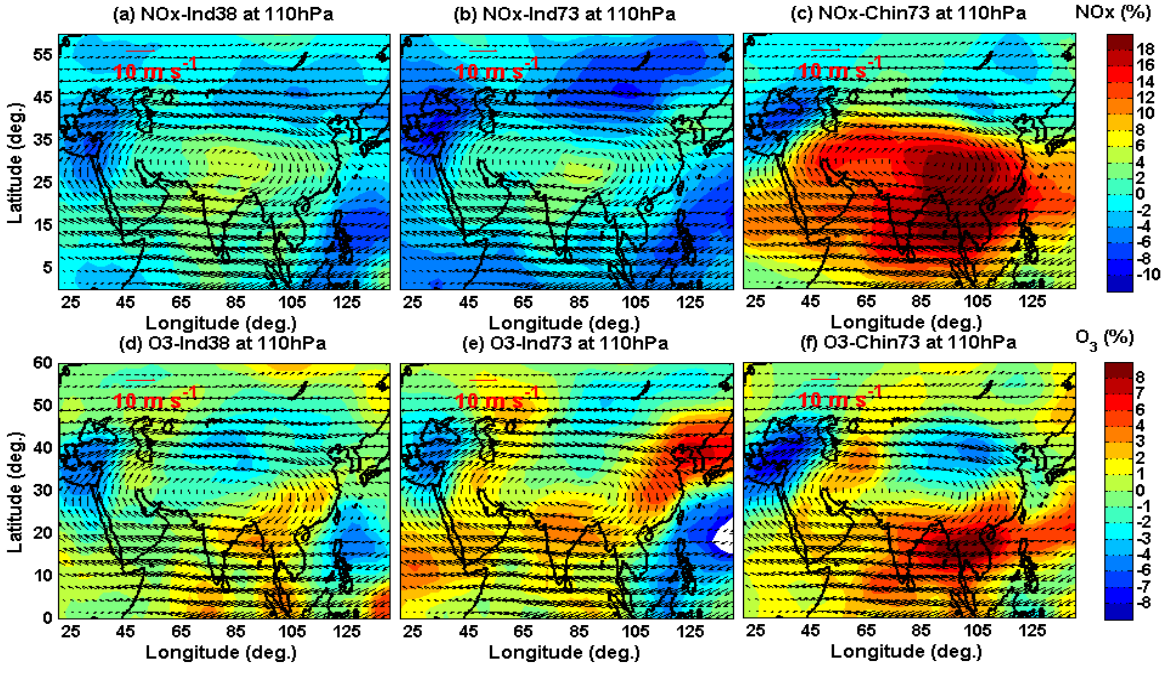

Figure 5: Latitude-longitude cross-section of NO_x anomalies (%) averaged for the monsoon season (June-September) at 110 hPa obtained from (a) Ind38 (b) Ind73 (c) Chin73 simulations. (d-f) Show the same but for ozone (%) at 110 hPa for (d) Ind38 (e) Ind73 (f) Chin73 simulations. Black arrows indicate horizontal winds at 110 hPa.

Atmos. Chem. Phys. Discuss., doi:10.5194/acp-2016-582, 2016
Manuscript under review for journal Atmos. Chem. Phys.
Published: 20 July 2016

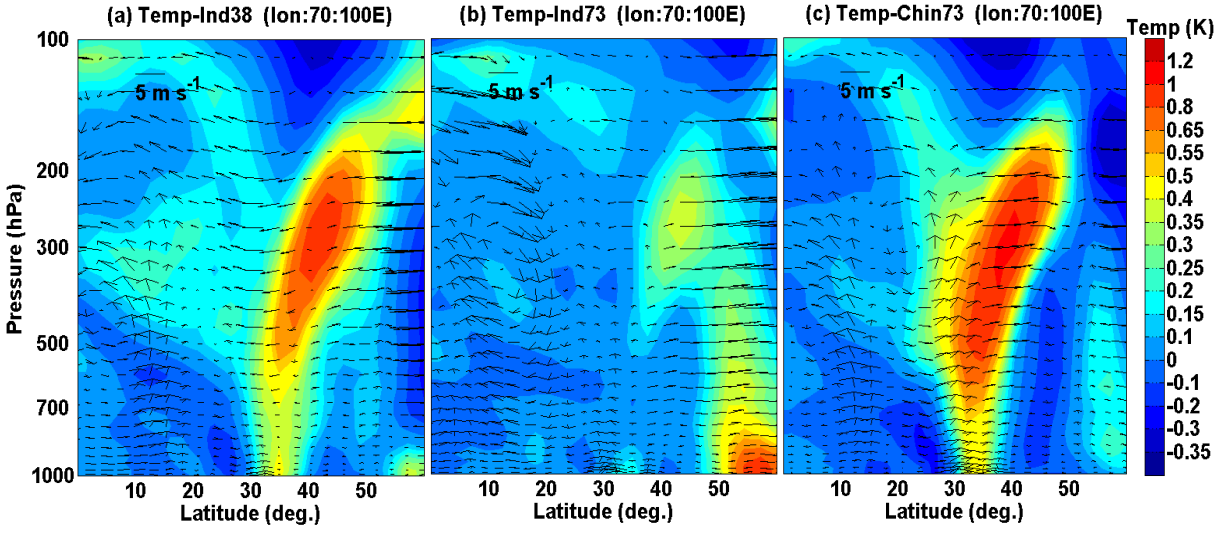

Figure 6: Latitude pressure cross-section of temperature anomalies (K) averaged for the monsoon season (June-September) obtained from (a) Ind38 (averaged over 70ºE-94ºE) (b) Ind73 (averaged over 70ºE-94ºE) and (c) Chin73 (averaged over 70ºE-100ºE) simulations. Black arrows indicate wind vectors. The vertical velocity field has been scaled by 300.

Atmos. Chem. Phys. Discuss., doi:10.5194/acp-2016-582, 2016
Manuscript under review for journal Atmos. Chem. Phys.
Published: 20 July 2016

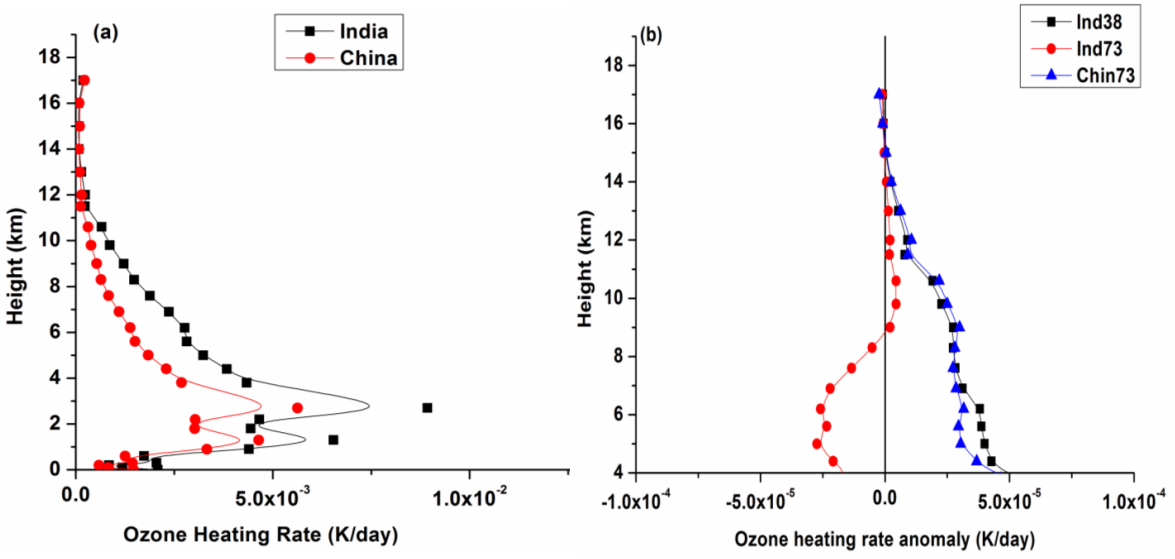

Figure 7: Vertical profile of (a) ozone heating rate (K/day) obtained from CTRL simulations averaged over India (70º-94ºE, 20º-30ºN) and China (70º-100ºE, 30º-40ºN), (b) ozone heating rate anomaly(K/day) averaged over Tibetan Plateau (70º-100ºE, 20º-30ºN) obtained from Ind38, Ind73 and Chin73 simulations.

Atmos. Chem. Phys. Discuss., doi:10.5194/acp-2016-582, 2016
Manuscript under review for journal Atmos. Chem. Phys.
Published: 20 July 2016

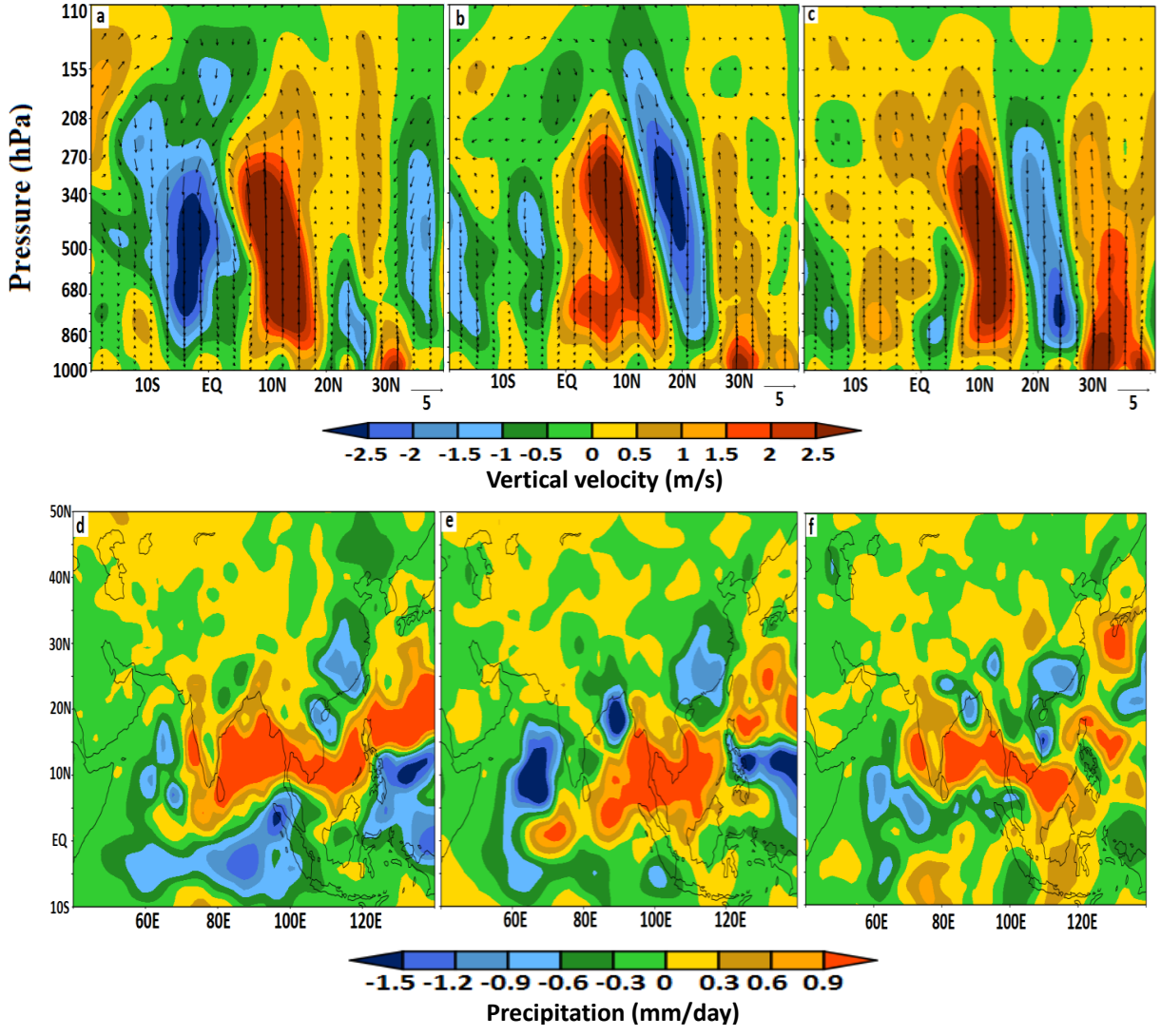

Figure 8: Change in the meridional circulation due to enhanced NO_X emissions averaged for the monsoon season (June-September) and over 70ºE-110ºE for (a) Ind38 (b) Ind73 (c) Chin73 simulations. Shaded contours indicate the anomalies in vertical velocity (m/s). The vertical velocity field has been scaled by 300. Precipitation anomalies (mm/day) averaged for the monsoon season (June-September) obtained from (d) India38 (e) Ind73 (f) Chin73 simulations with respect to CTRL.